DOI: 10.1002/cphc.200700863

Mechanism-Guided Improvements to the Single Molecule Oxidation of Carbon Nanotube Sidewalls

John G. Coroneus,[b] Brett R. Goldsmith,[a] Jorge A. Lamboy,[c] Alexander A. Kane,[a] Philip G. Collins,*[a] and Gregory A. Weiss*[b, c]

Real-time monitoring of carbon nanotube conductance during electrochemical and chemical etching reveals the electronic signatures of individual bond alteration events on the nanotube sidewall. Tracking the conductance of multiple single-molecule experiments through different synthetic protocols supports putative mechanisms for sidewall derivatization. Insights gained from these mechanistic observations imply the formation of sidewall carboxylates, which are useful as handles for bioconjugation. We describe an electronic state required for efficacious chemical treatment. Such real-time monitoring can improve carboxylate yields to 45% or more. The experiments illustrate the power of molecular nanocircuits to uncover and direct the mechanisms of chemical reactions.

1. Introduction

Characterization of carbon nanotube reactivity represents a key step for the implementation of advanced biomolecular electronic devices. Recently, we have demonstrated precise chemical control over sidewall functionalization using nanotube circuits as a tool to investigate and steer chemical reactivity.[1] In these experiments, a single-walled nanotube (SWNT) wired to connective electrodes and monitored for electrical conductance allows the production of individual sidewall defects. Further derivatization of these sites is possible, though with a low experimental yield, and the creation of carboxylic terminations are experimentally difficult. In principle, however, the conductance signal allows reaction progress to be monitored and even controlled, for example by indicating the appropriate time to reduce the electrochemical potential or change the chemical solution.

This paper builds upon our recent communication[1] to provide detailed, improved procedures and an investigation of the conductance dynamics taking place during modification of SWNT sidewalls. In particular, experiments with a large number of devices have identified distinct signatures required for the successful incorporation of a carboxylate defect. The observations lead to a proposed mechanism for sidewall oxidation at single-molecule levels. Given the stochastic nature of single-molecule reactions, and the difficulty of performing traditional assays like spectroscopy on such systems, conductance tracking allows more consistent syntheses and higher yields. The results illustrate the potential of molecular circuits for uncovering mechanistic details of chemical reactions and guiding reactions to form useful hybrid devices that might otherwise have very low yields.

Functionalities on nanotube sidewalls are critical to the fabrication of hybrid, nanotube-based composites for fuel cells, biosensors, catalyst supports, and supercapacitors.[2] Specifically, incorporation of carboxylates often requires treatment with acid using long exposure times, and elevated temperatures.[3] When assayed, bulk materials exhibit various functional groups including carboxylates, hydroxyls, epoxides, and ketones, with the exact location—on sidewall or SWNT ends—usually remaining ambiguous.[3–7] Careful analysis of bulk oxidation of carbon nanotubes,[8–10] and studies of high quality graphites[11,12] indicate the formation of epoxide and hydroxyl functionalities on nanotubes and on the graphite basal plane. On graphite, carboxylic acid groups produced by chemical oxidation are located primarily at step edges.[11] On SWNTs, such functionalities are initially produced on nanotube ends or end caps and at defects incorporated during growth; only further oxidation can etch sidewalls.[4,6–8,13–15] The latter results illustrate the difficulty of converting SWNT sidewalls into carboxylates or ketones. Careful control of the oxidative process is needed to overcome the sidewall resistance to carboxylate formation while maintaining its electrical conductivity.

2. Results and Discussion

To optimize the production of working circuit elements that contain carboxyl groups for bioconjugation, our chemical in-

[a] *B. R. Goldsmith, A. A. Kane, Prof. P. G. Collins*
Department of Physics and Astronomy
University of California, Irvine, California 92697-2025 (USA)
Fax: (+1) 949-824-2174
E-mail: collinsp@uci.edu

[b] *J. G. Coroneus, Prof. G. A. Weiss*
Department of Molecular Biology and Biochemistry
University of California Irvine, California 92697-2025 (USA)
Fax: (+1) 949-824-9920)
E-mail: gweiss@uci.edu

[c] *J. A. Lamboy, Prof. G. A. Weiss*
Department of Chemistry
University of California, Irvine, California 92697-2025 (USA)

Supporting information for this article is available on the WWW under http://www.chemphyschem.org or from the author.

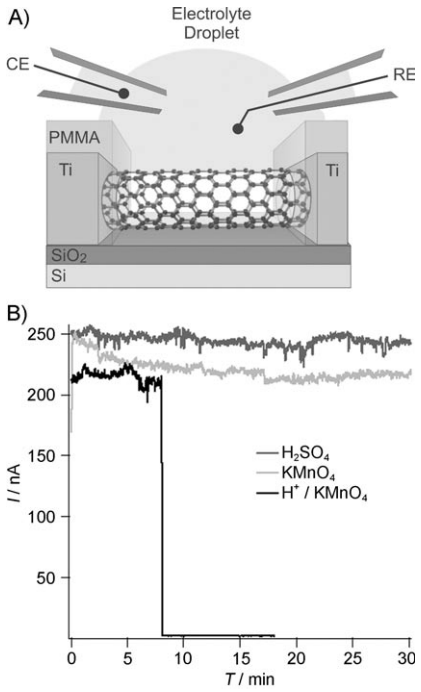

Figure 1. A) Schematic of the device setup showing SWNT, electrodes (either Ti or Pd), and PMMA coating. In the liquid, Pt electrodes, either bare or integrated into capillaries (shown), control and monitor the electrochemical potential. B) Stability of a device in H_2SO_4, $KMnO_4$ (aq) and $KMnO_4$ (acidic). Acidic $KMnO_4$ does etch the SWNT, but only after 8 min—significantly longer than the 30 s chemical treatments used here.

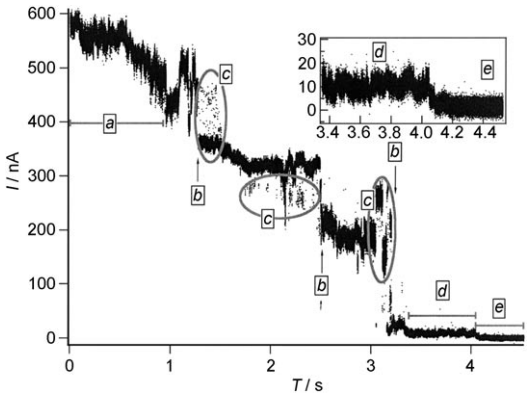

Figure 2. A typical electrochemical oxidation of a SWNT (0.83 V versus Pt), showing steps *a* through *e*. Inset: a magnified section of the data with the device remaining in *d* from 3.4 to 4.1 seconds. Arrows indicate the sharp drop characteristic of *b*; grey ellipses emphasize the bistability of *c*, and grey horizontal bars serve as guides to *d* and *e*. Further examples of SWNT oxidations are given in the Supporting Information.

vestigations specifically target clean SWNT sidewalls using an electronic device architecture depicted in Figure 1 A, and described previously.[1,16] Devices consist of isolated SWNTs, either metallic or semiconducting, sparsely grown on SiO_2 by chemical vapor deposition and connected to Ti photolithographic electrodes. By coating each device with a protective layer of PMMA and then using electron beam lithography to open a small (<1 μm) window to the SWNT sidewall, reagent exposure is effectively controlled, limiting oxidation–reduction reactions to the SWNT sidewall. Alternately, titanium electrodes with a passivating native oxide are used in an analogous manner, diminishing the requirement for a PMMA coating.[1,17] An electrochemical fluid cell controls reagents in contact with the SWNT, while SWNT conductance (*G*) is independently monitored using a 100 mV potential (Figure 1 A). This approach maintains a functioning electronic device while allowing chemistry to take place on the nanotube sidewall, with previous reports proving the utility of the method.[1,16] For example, the onset of sidewall derivatization is clearly observed as *G* decreases when electrochemical potentials are used to promote oxidation (Figure 2). Theoretical models link the decrease in conductance with sp^2 to sp^3 rehybridization of sidewall carbons.[18] Upon electrochemical reduction, chemical functionalities can return the sp^3-hybridized carbons of the sidewall to an sp^2 hybridization state.

Herein we investigate the conditions that lead to irreversible drops in *G* from the starting conductance (G_0). Reduction will not return *G* to G_0 if carbons have been removed from the SWNT lattice (e.g. through formation of carboxylates or esters). Acidic electrochemical conditions are used for comparison to the extensive studies of graphite[19] and bulk SWNT[8,20–23] oxidation, where long exposures to similar oxidative conditions are typical. Yet such conditions can easily lead to overoxidation in single molecule SWNTs. Figure 1 B demonstrates the stable *G* of the SWNT device configuration exposed to oxidizing agents ($KMnO_4$) and acids (H_2SO_4) at room temperature without the application of an electrochemical potential. Thus, we conclude that short exposures to these chemicals are insufficient to introduce functionalities leading to decreased conductance in pristine SWNT sidewalls.

Oxidation proceeds in a few seconds when moderate electrochemical potentials are applied using the identical solutions. Oxidation experiments reveal variable elements in the resultant conductance drops, which are characteristic of the unpredictable behavior expected from single-molecule observations. A representative sample of oxidation profiles to illustrate such variations is given in the Supporting Information Figure S1. Reproducible features from sample to sample exist, and are labeled *a* through *e* in Figure 2 and Supporting Information Figure S1. Putative mechanistic steps corresponding to each reproducible feature have analogous labels in Figure 3.

In Figure 2, the decrease in *G* labeled *a* corresponds to the "overcharging" stage observed in experiments with bulk nanotubes and graphites.[19,22] A continuous, monotonic drop in *G* is observed, and likely corresponds to the buildup of positively charged scattering centers in intermediate **2**. "Overoxidation" occurs when the doping progresses beyond a critical concentration of approximately one positive charge for every 21 carbons (C_{21}^+)[19], leading to sp^3 rehybridization of the sidewall carbons as conjugate bases covalently add to the carbon lattice. In SWNTs, these covalent events, *b*, cause abrupt drops in *G* of 10-50 %. Many events are accompanied by multiple, rapid reversals, *c*. This high-speed dynamic between intermediates **2** and **3** is consistent with a model in which the conjugate base remains in close proximity to the surface; the covalent bond to

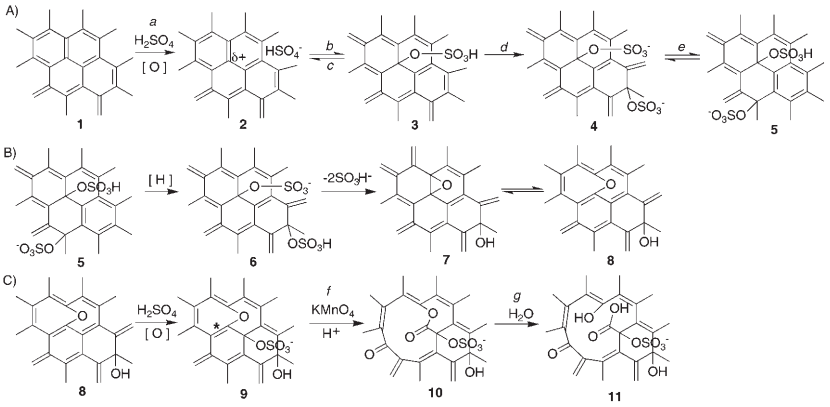

Figure 3. Proposed mechanism of a carbon nanotube subjected to electrochemical A) oxidation ([O]), B) reduction ([H]), C) subsequent additional oxidation ([O]) and chemical treatment with $KMnO_4$ in the absence of an electrochemical potential (steps *f* and *g*). The lettered mechanistic steps putatively correspond to electronic signatures with analogous labels in Figure 2. The carboxylate in **11** could be used for bioconjugation. 1,2-additions are sterically strained (see Supporting Information Figure S2). * in **9** indicates an electron rich, non-aromatic olefin, which is more susceptible to oxidation. This mechanism with incorporation of an oxygen into the sidewall scaffold accounts for the greatly enhanced sensitivity of SWNT sidewalls after >1 oxidation–reduction cycles.

the SWNT breaks and reforms as addition–elimination reactions compete thermodynamically.

Ultimately, a SWNT always stabilizes into a low-*G*, oxidized state, *d*, an electronic signature not carefully controlled in our earlier work. The real-time observation of equilibration before reaching *d*, however, indicates the diversity of adduct stabilities. Furthermore, a device at *d* will continue to exhibit metastability until a final, ~1% drop to zero conductance, *e*. Achieving the electronic signature observed in transitioning from *d* to *e* requires a constant oxidizing potential: lowering the potential returns the device to *d*. Thus, the formation of intermediate **5** is likely a physical rearrangement of adducts driven by electrostatics and aromaticity—the clustering of separated adducts in going from intermediates **4** to **5** can reduce the number of non-aromatic hexagonal rings, but simultaneously generate an electronic barrier that is physically wider and energetically deeper.

Electrochemical reduction can restore conductance to levels greater than or equal to 0.95 G_0[1,16] from any of the electronic signatures labeled *a* through *e*, provided the device is not treated with $KMnO_4$. This restored state, which can also be obtained by heating to 450 °C in Ar, indicates the presence of reducible functionalities attached to a sp^3-hybridized carbon. Conversely, groups like carboxylates resulting from breakup of the SWNT lattice result in permanent modification.[24] Reduction also leads to formation of epoxide **7**, which can quickly rearrange to ether **8**. Curvature of the nanotube sidewall favors this rearrangement.[18]

Figure 4 shows results from 45 single-molecule nanocircuits, and shows that only one device in 25 (4%) fails to recover after a full oxidation–reduction cycle in 1 M H_2SO_4. This high rate of recovery demonstrates that H_2SO_4 etching, both alone and in conjunction with electrochemical oxidation, is insufficient to cause permanent modification to the SWNT sidewall lattice. By comparison, chemical oxidation protocols on bulk nanotubes include longer reaction times, elevated temperatures, and sonication, all of which expedite sidewall oxidation.[6–8,14] Another 20 devices were oxidized with the addition of 6.5 mM acidic $KMnO_4$ solution when the device achieved electronic state *d* or *e*. With application of $KMnO_4$, the rate of permanent modification increases to four of 20 devices (20%). Treatment with $KMnO_4$ appears to have no effect on the conductance of devices oxidized only to *d*, as these devices all recovered to nearly G_0 (four of four). This is a surprising result given that chemical treatments of bulk nanotubes with $KMnO_4$ result in carboxylate formation.[14] In our experiments, permanent modification required treatment with $KMnO_4$ after reaching state *e*, (four of 16). We conclude that the yield of permanent modifications can be driven as high as 25% in a single oxidation-reduction cycle, provided care is taken to always attain *e*.

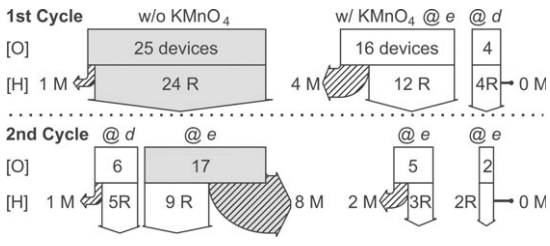

Figure 4. SWNT device treatments. Grey areas indicate the most efficient synthetic protocol, and diagonal markings indicate experiments leading to permanently modified devices. R = devices with significant recovery in conduction; M = permanently modified devices. On the left, [H] and [O] indicate electrochemical reduction and oxidation, respectively. Notation above the block arrows *@d* and *@e* indicate the electronic signature attained before addition of an acidic solution of $KMnO_4$.

Since most devices exhibit a high degree of recovery, multiple electrochemical cycles can be used. Figure 4 demonstrates that the yield of permanent modifications dramatically increases on the second oxidation cycle. Specifically, application of $KMnO_4$ upon attaining state *e* results in permanent modification of eight of 17 devices previously cycled in acid. Five of the devices that recovered on reduction in spite of the application of $KMnO_4$ at *e* in the first oxidation cycle were subjected to a second oxidation at *e* followed by $KMnO_4$ treatment. Of these, two were permanently modified. In total, 10 of the 22 devices that were subjected to two oxidations plus $KMnO_4$ treatment were permanently modified, for a total yield of 45%. This yield is nearly twice the best result observed with a single oxidation cycle. Functional groups introduced during the first cycle are key to promoting attack by the $KMnO_4$, analogous to the preferential oxidation at growth defects. As with the first oxidation cycle, application of $KMnO_4$ at state *d* is not effective at modi-

fying the SWNT, even when applied on the second oxidation cycle.

Thus, we identify two important aspects in the production of permanent modifications like carboxylates. First, *d* is a unique electronic state, distinct from *e*, and devices at *d* are much less susceptible to attack by $KMnO_4$—independent of previous oxidation. Second, we observe that $KMnO_4$ attack, while still less than 100% efficient, is more effective on SWNTs with pre-existing disorder. Figure 3 combines these observations into a proposed mechanism for the production of carboxylates—the dominant product seen previously.[1] The first oxidation–reduction cycle is believed to incorporate an ether oxygen into the SWNT sidewall[1] (Figures 3A and B, intermediate **8**), increasing the susceptibility of the device to subsequent oxidation. The non-planar oxygen of the ether in intermediate **8** decreases the aromatic stability of the adjacent rings, making their carbons more susceptible to sulfate addition. In turn, the resultant, non-aromatic ring has greater electron density (* in intermediate **9**, Figure 3C) for attack on the electrophilic MnO_4^-.

3. Conclusions

The reported experiments illuminate some most difficult observations in organic chemistry—formation of intermediates, transition states, and establishment of equilibria. Monitoring the electronic signature throughout the process traces reaction progress, and allows observation of such intermediates, though presently limited to 10 μs resolution. Having linked carboxylate formation to a permanent decrease in *G*, the production of carboxylates on a SWNT can now be driven above 90% by cycling two or more times until the desired signal is observed. This procedure enables device preparation for further chemical and biological experiments.

Acknowledgements

The authors gratefully acknowledge technical assistance from V. Khalap and T. Sheps, support from NSF (EF-0404057, DMR-0239842 and CHE-0533162) and a CalIT2 Emulux Fellowship.

Keywords: bioconjugation · molecular electronics · nanotubes · oxidation · single-molecule studies

[1] B. R. Goldsmith, J. G. Coroneus, V. R. Khalap, A. A. Kane, G. A. Weiss, P. G. Collins, *Science* **2007**, *315*, 77–81.
[2] R. H. Baughman, A. A. Zakhidov, W. A. de Heer, *Science* **2002**, *297*, 787–792.
[3] A. Hirsch, O. Vostrowsky in *Functional Molecular Nanostructures* (Ed.: A. D. Schluter), Springer, Heidelberg, **2005**.
[4] S. Banerjee, T. Hemraj-Benny, S. S. Wong, *Adv. Mater.* **2005**, *17*, 17–29.
[5] R. J. Chen, S. Bangsaruntip, K. A. Drouvalakis, S. K. N. Wong, M. Shim, Y. Li, W. Kim, P. J. Utz, H. Dai, *Proc. Natl. Acad. Sci. USA* **2003**, *100*, 4984–4989.
[6] H. Hiura, T. W. Ebbesen, K. Tanigaki, *Adv. Mater.* **1995**, *7*, 275–276.
[7] S. Niyogi, M. A. Hamon, H. Hu, B. Zhao, P. Bhowmik, R. Sen, M. E. Itkis, R. C. Haddon, *Acc. Chem. Res.* **2002**, *35*, 1105–1113.
[8] S. Lefrant, I. Baltog, M. Baibarac, *J. Raman Spectrosc.* **2005**, *36*, 676–698.
[9] K. J. Ziegler, Z. Gu, J. Shaver, Z. Chen, E. L. Flor, D. J. Schmidt, C. Chan, R. H. Hauge, R. E. Smalley, *Nanotechnology* **2005**, *16*, S539.
[10] K. J. Ziegler, Z. Gu, H. Peng, E. L. Flor, R. H. Hauge, R. E. Smalley, *J. Am. Chem. Soc.* **2005**, *127*, 1541–1547.
[11] A. Lerf, H. He, M. Forster, J. Klinowski, *J. Phys. Chem. B* **1998**, *102*, 4477–4482.
[12] S. Stankovich, R. D. Piner, X. Chen, N. Wu, S. T. Nguyen, R. S. Ruoff, *J. Mater. Chem.* **2006**, *16*, 155–158.
[13] N. Zhang, J. Xie, V. K. Varadan, *Smart Mater. Struct.* **2002**, 962.
[14] J. Zhang, H. Zou, Q. Qing, Y. Yang, Q. Li, Z. Liu, X. Guo, Z. Du, *J. Phys. Chem. B* **2003**, *107*, 3712–3718.
[15] P. M. Ajayan, T. W. Ebbesen, T. Ichihashi, S. Iijima, K. Tanigaki, H. Hiura, *Nature* **1993**, *362*, 522–525.
[16] J. Mannik, B. R. Goldsmith, A. Kane, P. G. Collins, *Phys. Rev. Lett.* **2006**, *97*, 016601.
[17] I. Heller, J. Kong, H. A. Heering, K. A. Williams, S. G. Lemay, C. Dekker, *Nano Lett.* **2005**, *5*, 137–142.
[18] Y.-S. Lee, N. Marzari, *Phys. Rev. Lett.* **2006**, *97*, 116801–116804.
[19] K. Kinoshita, *Carbon—Electrochemical and Physicochemical Properties*, Wiley-Interscience, New York, **1988**.
[20] M. Burghard, *Surf. Sci. Rep.* **2005**, *58*, 1–109.
[21] R. Graupner, J. Abraham, A. Vencelova, T. Seyller, F. Hennrich, M. M. Kappes, A. Hirsch, L. Ley, *Phys. Chem. Chem. Phys.* **2003**, *5*, 5472–5476.
[22] G. U. Sumanasekera, J. L. Allen, S. L. Fang, A. L. Loper, A. M. Rao, P. C. Eklund, *J. Phys. Chem. B* **1999**, *103*, 4292–4297.
[23] S. Lefrant, I. Baltog, M. Baibarac, J. Y. Mevellec, O. Chauvet, *Carbon* **2002**, *40*, 2201–2211.
[24] S. Stankovich, D. A. Dikin, G. H. B. Dommett, K. M. Kohlhaas, E. J. Zimney, E. A. Stach, R. D. Piner, S. T. Nguyen, R. S. Ruoff, *Nature* **2006**, *442*, 282–286.

Received: January 26, 2008
Revised: March 14, 2008
Published online on April 8, 2008

